Composite Columns Reinforced with Rebars and Embedded I-Sections Made of Steel or GFRP: An Experimental Approach

Wed Hussein Habeeb
Department of Civil Engineering, College of Engineering, University of Baghdad, Baghdad, Iraq
wid.habib2201m@coeng.uobaghdad.edu.iq (corresponding author)

Ali Hussein Ali Al-Ahmed
Department of Civil Engineering, College of Engineering, University of Baghdad, Baghdad, Iraq
dr.ali-alahmed@coeng.uobaghdad.edu.iq

Received: 14 May 2025 | Revised: 28 June 2025 and 10 July 2025 | Accepted: 11 July 2025

 DOI: https://doi.org/10.48084/etasr.12129

ABSTRACT

This study experimentally investigates the structural performance of reinforced concrete columns incorporating steel and/or Glass Fiber Reinforced Polymer (GFRP) bars and I-sections under concentric loading. Six square columns (170 mm × 170 mm cross-section and 1500 mm height) with a compressive strength of 30.25 MPa were tested. Three reinforcement schemes were used: hybrid (GFRP I-sections with steel bars and vice versa), homogeneous (GFRP or steel I-sections with corresponding bars), and reference (bars only). A novel reinforcement technique employed four longitudinal I-sections with bars. The results indicate that the columns with I-sections outperformed the reference ones, with steel I-sections showing the highest capacity. The steel reference column exhibited 10.18% higher strength than its GFRP counterpart; the large steel I-section columns outperformed the GFRP ones by 57%, and the small steel I-section columns by 38%. This study highlights the potential of GFRP as a corrosion-resistant alternative in structural applications.

Keywords-Glass Fiber-Reinforced Polymer (GFRP); composite column; GFRP I-sections; steel I-sections; concentric load

I. INTRODUCTION

The use of Fiber-Reinforced Polymer (FRP) bars as an alternative to traditional steel reinforcement in concrete structures has grown steadily, owing to the advantageous properties of FRP, such as its high tensile strength and exceptional resistance to corrosion [1]. GFRP bars have been increasingly adopted over the past two decades as replacements for steel. Advancements in FRP technology have produced GFRP bars with elastic moduli exceeding 60 GPa, allowing for a reduction in the quantity of reinforcement required and contributing to more cost-effective structural designs. These bars are manufactured with various surface textures, including smooth, deformed, sandblasted, and grooved finishes to improve the bond strength with the surrounding concrete [2]. One of the principal challenges associated with steel reinforcement is its susceptibility to corrosion, especially in coastal environments and other aggressive conditions. The resulting deterioration can significantly impair the structural integrity and lead to high maintenance and repair costs. In response, FRP bars have emerged as corrosion-resistant alternatives to steel [3]. Extensive research has been devoted to the use of GFRP in structural elements, particularly in the form of I-sections used in composite beams. According to [4], GFRP bars are well-suited for construction applications due to their lightweight nature, high tensile capacity, and minimal maintenance requirements. Authors in [5] evaluated the behavior of GFRP bars under elevated temperatures and harsh environmental conditions, concluding that their use can effectively mitigate the fire-related damage in reinforced columns. Authors in [6] focused on eccentrically loaded concrete columns reinforced with GFRP. The results demonstrated that increasing GFRP thickness led to higher ultimate load capacities, although this benefit diminished as the load deflection increased. Similarly, authors in [7] reported that composite columns utilizing either steel or GFRP I-sections exhibited higher load capacities than their unreinforced counterparts. However, replacing the steel I-sections with GFRP in such columns tended to reduce the ultimate strength under concentric loading. Despite their favorable characteristics, such as high stress tolerance, low maintenance, and reduced weight, FRP materials have seen limited adoption in some sectors [8]. There remains a notable gap in research concerning hybrid columns that integrate both steel and GFRP reinforcement.

Authors in [9] introduced a 1% volume fraction of GFRP and steel to concrete mixes and found significant improvements in the mechanical performance, but only minor increases in the compressive strength. Further comparisons between longitudinal GFRP and steel bars in hollow square concrete columns were made in [10], where it was shown that GFRP-reinforced columns exhibited lower load capacities than their steel-reinforced counterparts. Similarly, authors in [11] examined the flexural response of concrete slabs reinforced with GFRP bars, revealing a bilinear elastic behavior with a marked reduction in stiffness following the crack formation. The experimental results from [12] indicated that the ductility index of composite beams increased significantly compared to the control specimens by 156.2% when using GFRP and shear connectors, 148.6% with GFRP alone, and 96% with steel I-sections. A numerical study in [13] highlighted that GFRP- and hybrid-reinforced columns dissipated only 0.42 and 0.75 times, respectively, the energy of steel-reinforced columns. Authors in [14] examined hybrid columns reinforced longitudinally with both steel and GFRP bars, noting improvements in the load capacity and post-peak behavior, while also maintaining the corrosion resistance benefits of GFRP. Similar conclusions were reached in [15], where square columns reinforced longitudinally and transversely with GFRP, displayed a comparable performance to that of the steel-reinforced specimens, albeit with slightly reduced ductility and stiffness losses. Consistent results were obtained in [16], while in [17], it was demonstrated that GFRP reduces the plastic creep and enhances the flexural stability in axially tensioned members. In [18], the addition of a helical GFRP confinement was found to increase both the ductility and axial load capacity by 12%–18%. Authors in [19] reported that encasing concrete in GFRP tubes significantly improved the confinement and post-peak behavior, although the stiffness remained lower than that of the steel-encased columns. The durability of GFRP under environmental stressors, such as humidity, heat, and electric fields was confirmed in [20], with minimal degradation in material properties over time. In terms of the structural rehabilitation, authors in [21] explored the use of extruded GFRP profiles for retrofitting damaged lattice steel columns. It was revealed that all retrofitted columns, whether repaired with angles or GFRP-steel bolted systems shared similar failure modes with the original configuration, confirming the effectiveness of the GFRP reinforcement. Authors in [22] evaluated eight concrete-encased composite columns under cyclic axial loads to simulate the seismic activity. The findings highlighted the excellent seismic resilience of these columns, making them suitable for both seismic and non-seismic regions due to their high strength and load-repetition capacity. Finally, authors in [23] conducted an in-depth analysis of the mechanical behavior of GFRP-reinforced concrete columns, concluding that while the FRP bars exhibit superior tensile and compressive strengths compared to the steel ones, their compressive strength is typically around 70% of their tensile strength. Supporting this, authors in [24] found that columns reinforced with GFRP showed stable cyclic performance and only a slight reduction in strength relative to the steel-reinforced columns.

II. EXPERIMENTAL PROGRAM

A. Tested Specimens

Six reinforced concrete columns were built and classified into three types based on the presence of I-sections. The first group includes two columns: one with steel bars and four steel I-sections (B.I-S), and the second with GFRP bars and four GFRP I-sections (B.Ig-Gb). The second group also has two composite columns: one with steel bars and four GFRP I-sections (B.Ig-Sb), and another with GFRP bars and four steel I-sections (B.Is-Gb). The last group comprises two reference columns without I-sections, containing only bars, one with steel bars (Sb) and the other with GFRP bars (Gb). These specimens were designed, cast, and tested under central loading. All specimens had the same reinforcement, including four Ø10mm steel or GFRP longitudinal bars with Ø6mm @150 mm steel ties. For both the steel and GFRP I-sections, the cross-sectional area of one section was the same (50 mm × 25 mm × 4 mm). All specimens were 1500 mm high and 170 mm wide, forming a square. The details of the columns are shown in Figures 1, 2, and Table I.

TABLE I. DETAILS OF TEST SPECIMENS

Group	Specimen	Type of rebars	Type of I-section
G1	$B.I_S$-S_b	Steel	Steel
	$B.I_g$-G_b	GFRP	GFRP
G2	$B.I_S$-G_b	GFRP	Steel
	$B.I_g$-S_b	Steel	GFRP
G3	S_b	Steel	-----
	G_b	GFRP	-----

B.Is-Sb refers to I-section steel with steel bars, B. Ig-Gb refers to I-section GFRP with GFRP bars, B.Is-Gb refers to I-section steel with GFRP bars, and B.Ig-Sb refers to I-section GFRP with steel bars. Sb refers to a column with I-section only steel bars, and Gb refers to a column without I-section only GFRP bars.

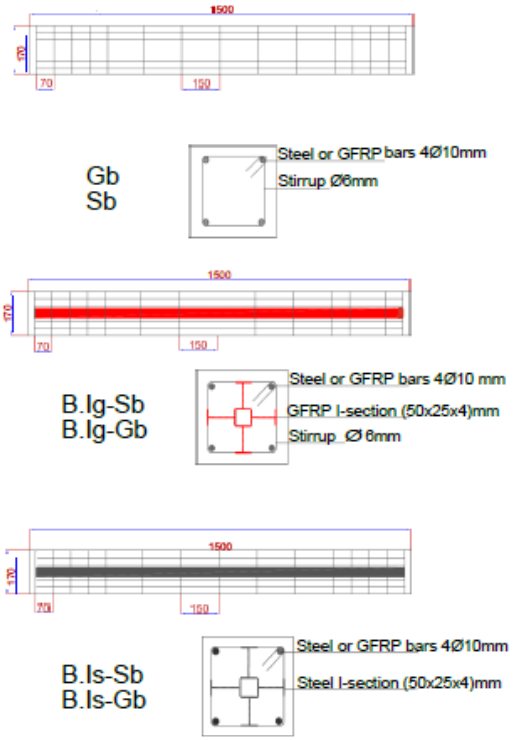

Fig. 1. Specimen details (all dimensions are in mm).

Fig. 2. Reinforcement cage for GFRP and steel I-sections.

B. Material Properties

1) Concrete

The study required making concrete of normal strength. It was cast using a central mixer. Column specimens were produced with an average cylindrical compressive strength of 30.25 MPa; the mixture consisted of cement, natural sand, fine aggregate with a gradation of 5 mm - 12 mm that was crushed, water, and superplasticizing accelerator additives added at a rate of 3 L. Six standard 150 mm cube-shaped test samples were obtained. The aim of taking these samples was to verify the average compressive strength of the concrete used. Table II lists the proportions of the normal-strength concrete utilized in the concrete mix.

TABLE II. CONCRETE MIX PROPORTIONS

Mix proportion (kg/m^3)				
Gravel	**Cement**	**Sand**	**Water**	**Additive**
1060	450	800	85 L	3 L

2) GFRP and Steel Bars

The steel reinforcement bars used in this study had a diameter of 10 mm and a length of 1450 mm, with a yield strength of 338.4 MPa, an ultimate tensile strength of 428.4 MPa, and an elongation of 22%, as determined through tensile testing, using standard steel coupons. The GFRP bars, also 10 mm in diameter, had an ultimate tensile strength of 900 MPa and a modulus of elasticity ranging from 46 to 60 GPa, according to the manufacturer data. The mechanical properties of both types of bars are summarized in Table III.

TABLE III. MECHANICAL PROPERTIES OF GFRP AND STEEL REINFORCEMENT

Type	**Diameter (mm)**	**Length (mm)**	**Mass (gm)**	**Yield strength (MPa)**	**Ultimate strength (MPa)**	**Elongation (%)**
Steel	10	440.3	224.7	338.4	428.4	22
GFRP	10	1450	20.88	….	900	….

3) GFRP I-Section Properties

GFRP structural 50 mm × 25 mm × 4 mm I-sections were ordered due to their unavailability locally. Table IV illustrates the characteristics of the global control system as stated in the inspection report submitted by the supplier.

TABLE IV. MECHANICAL PROPERTIES OF GFRP SECTIONS

GFRP profile	**Size (mm)**	**Tensile strength (MPa)**	**Compressive strength (MPa)**	**Modulus of elasticity (MPa)**
I-Beam	50×25×4	681.57	350	40410

4) Steel I-Section Properties

The steel I-sections used in this study measured 50 mm × 25 mm × 4 mm. Since this specific size was not commercially available, the sections were custom fabricated for the research. A 4 mm thick steel plate was used to create the I-sections, with the components connected using welding wire. Tensile coupon samples were also prepared and tested, confirming that the fabricated sections met the required mechanical properties specified for steel plates, as shown in Table V [25].

TABLE V. MECHANICAL PROPERTIES OF STEEL PLATES

Coupon	**Thickness (mm)**	**Yield strength (MPa)**	**Ultimate strength (MPa)**	**Maximum elongation (%) in 50 mm**
Steel plate	3.4	344.9	436.7	68

C. Specimen Details

To aid in visualizing the crack formation during testing, all column specimens were painted white. The columns were tested 28 days after casting, under axial compression applied through fixed end supports. A 2000 kN load cell, positioned between the hydraulic jack and the loading head, was used to apply the load. Axial displacement was measured using a Linear Variable Differential Transformer (LVDT) installed at the base of the testing machine. Two solid steel loading heads, each 120 mm deep and 190 mm wide, were fixed to the top and bottom of the columns to ensure a uniform load distribution. A computerized data acquisition system recorded the applied loads and corresponding deformations. Figure 4 displays the test setup and equipment, while Figure 5 shows the specimens after mold removal and curing.

Fig. 3. Vertical LVDT (from the other side of the sample).

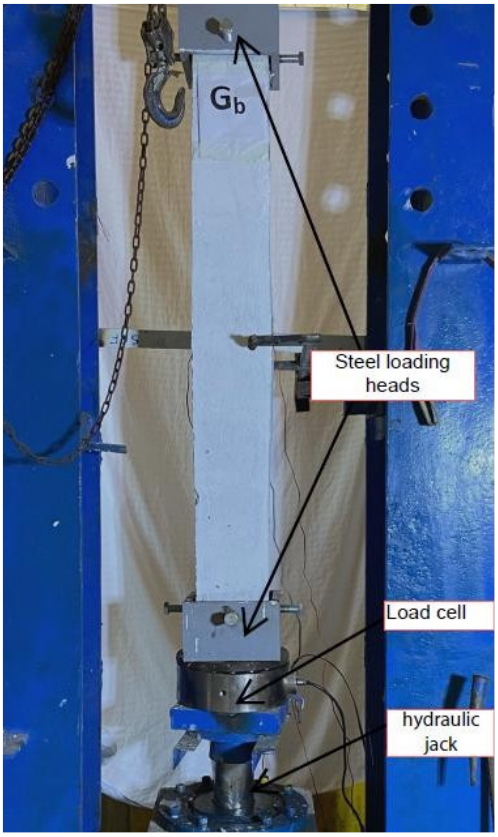

Fig. 4. Column test setup.

Fig. 5. The samples after mold opening and curing.

III. TEST RESULTS

A. Column Load Capacity

Table VI shows the difference in ultimate strength between the columns without sections and the columns with (steel or GFRP) under concentric loading. The tested specimens B.Is-Sb and B.Ig-Sb achieved ultimate strengths that were 58% and 9.7% higher than that of the reference specimen Sb, respectively. The tested specimens B.Ig-Gb and B.Is-Gb also achieved ultimate strengths that were 10.8% and 64% higher than that of the reference specimen Gb, respectively. The hybrid columns had higher ultimate strengths than those of the other columns. Steel-reinforced columns (B.Is-Sb) had the highest capacity (1386.9 kN), while hybrid columns (B.Ig-Sb and B.Is-Gb) exceeded the reference columns, indicating the contribution of I-sections.

TABLE VI. EXPERIMENTAL LOAD CAPACITY RESULTS

Group	Specimen	Ultimate load (KN)
G1	B.Is-Sb	1386.9
	B.Ig-Gb	883
G2	B.Is-Gb	1305.7
	B.Ig-Sb	963.8
G3	Sb	878.05
	Gb	796.88

B. Load-Deflection under Concentric Loading

The experimental results for the column samples are presented in Figures 6-8 for all tested specimens. To ensure that the load was centralized and that no failure or displacement occurred in the load location, a 120 mm deep and 190 mm wide steel box was fixed at the head and end of each column before testing. A maximum load of 883 kN was recorded for specimen B.Ig-Gb. After that, the load continued until a sudden failure occurred in the compression zone of the column specimen. B.Ig-Sb was the second specimen tested with a maximum load of 963.8 kN and B.Is-Sb was the third, with a maximum load of 1386.9 kN. This specimen achieved the highest ultimate load of all. B.Is-Gb was the fourth specimen tested, with a maximum load of 1305.7 kN, while Gb was the fifth, with a maximum load of 796.88 kN. Specimen Sb was tested last, reaching a maximum load of 878.05 kN.

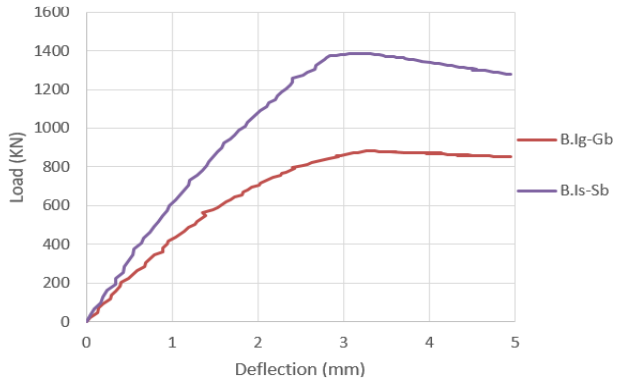

Fig. 6. Load-deflection curve of the B.Ig-Gb and B.Is-Sb specimen.

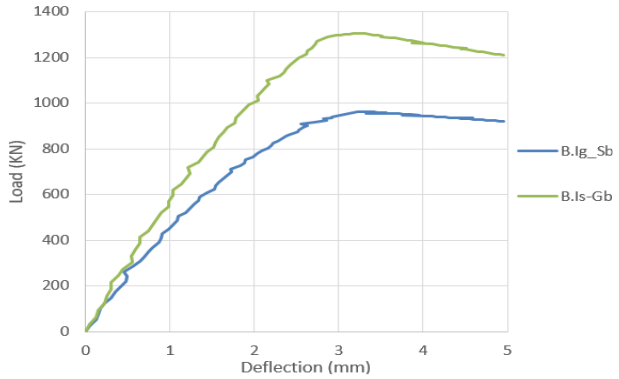

Fig. 7. Load-deflection curve of the B.Ig-Sb and B.Is-Gb specimen.

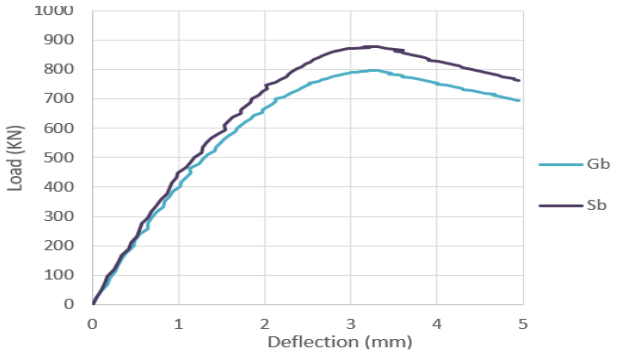

Fig. 8. Load-deflection curve of the Gb and Sb specimen.

C. Ductility and Energy Absorption

The ductility index was determined by calculating the ratio of the displacement at 85% of the post-peak load to the yield displacement. Among all specimens, the columns with steel I-sections exhibited the highest ductility. Energy absorption was evaluated as the area under the load–displacement curve. The specimen B.Is-Sb demonstrated the highest energy absorption, while B.Ig-Gb showed the lowest.

D. Stiffness

The initial stiffness was derived from the slope of the linear portion of the load-displacement curve. However, the post-yield stiffness was computed from the second slope after the yield point. Steel-reinforced columns exhibited higher stiffness in both phases.

E. Failure Modes

All column samples were tested up to failure, and different failure modes were observed depending on the type of reinforcement used. At the beginning of the test, all samples exhibited a similar behavior, with cracks initially developing at the top of the column. Cracks continued to expand to all sides of the sample as the test load was applied. Compression failure dominated most of the tested samples. Spalling was observed in the concrete cover of almost all samples due to the continuous and successive increase in the applied load. As for the reinforcement, denting was observed in the steel bars and sections, and tearing was also observed in the GFRP bars and sections. Table VII shows the failure modes for all tested column samples.

TABLE VII. FAILURE MODES

Specimen ID	Tested specimen	Failure mode
B.Is-Sb	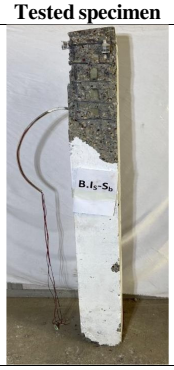	Compression failure mode. Peeling in the concrete cover. Minor dent in steel bars and sections.
B.Ig-Gb		Compression failure mode. Concrete cover fragmentation. Rupture in GFRP bars and sections. Tearing of steel ties
B.Is-Gb		Compression failure mode. Concrete cover fragmentation. Slight warping in the steel ties. Slight distortion in the steel section. Minor warping in GFRP bars.
B.Ig-Sb		Compression failure mode. Concrete cover fragmentation. Slight warping in the steel ties. Rupture of GFRP sections. Buckling of steel bars.
Sb		Compression failure mode. Concrete cover fragmentation. Warping in bars and steel ties.
Gb		Compression failure mode. Concrete cover fragmentation. Tearing of steel ties. Rupture and break in GFRP bars.

IV. CONCLUSIONS

This experimental study examined the structural behavior of composite reinforced concrete columns incorporating steel and/or Glass Fiber Reinforced Polymer (GFRP) longitudinal bars and I-sections under axial loading. A total of six columns with various reinforcement configurations, steel only, GFRP only, and hybrid were tested. The key findings are:

- The columns reinforced with I-sections showed a significantly greater load-bearing capacity compared to the reference columns without I-sections.
- The steel I-sections notably improved the ductility, energy absorption, and stiffness.
- The hybrid columns, combining steel and GFRP, outperformed the GFRP-only columns by offering a balance of strength and durability.
- The steel-reinforced reference column exhibited 10.18% higher strength than the GFRP reference column. The column with large steel I-sections surpassed its GFRP counterpart by 57%, while the column with small steel I-sections exceeded the GFRP version by 38%.

This study provides valuable insights into the synergistic behavior of steel and GFRP when used together as hybrid reinforcement. It also highlights GFRP's potential as a durable, corrosion-resistant material for reinforced concrete columns, while demonstrating the structural benefits of steel in enhancing the axial load performance. Future research should focus on assessing the long-term performance of these hybrid systems under cyclic loading and various environmental conditions to confirm their suitability for wider structural applications.

REFERENCES

[1] K. Khorramian and P. Sadeghian, "Experimental Investigation of Short and Slender Rectangular Concrete Columns Reinforced with GFRP Bars under Eccentric Axial Loads," *Journal of Composites for Construction*, vol. 24, no. 6, Dec. 2020, Art. no 04020072, https://doi.org/10.1061/(ASCE)CC.1943-5614.0001088.

[2] A. El-Nemr, E. A. Ahmed, A. El-Safty, and B. Benmokrane, "Evaluation of the flexural strength and serviceability of concrete beams reinforced with different types of GFRP bars," *Engineering Structures*, vol. 173, pp. 606–619, Oct. 2018, https://doi.org/10.1016/j.engstruct.2018.06.089.

[3] A. N. Tarawneh, H. M. Dwairi, G. S. Almasabha, and S. A. Majdalaweyh, "Effect of Fiber-Reinforced Polymer-Compression Reinforcement in Columns Subjected to Concentric and Eccentric Loading," *ACI Structural Journal*, vol. 118, no. 3, pp. 187–197, May 2021.

[4] M. Abdulkhaliq and A. H. Al-Ahmed, "The Flexural Behavior of One-Way Concrete Bubbled Slabs Reinforced by GFRP-Bars with Embedded Steel I-Sections," *Engineering, Technology & Applied Science Research*, vol. 14, no. 4, pp. 15860–15870, Aug. 2024, https://doi.org/10.48084/etasr.7680.

[5] M. H. Saeed and A. H. A. Al-Ahmed, "Properties of GFRP Bars Subjected to High Temperature," *Engineering, Technology & Applied Science Research*, vol. 15, no. 1, pp. 20012–20017, Feb. 2025, https://doi.org/10.48084/etasr.9710.

[6] A. Al-Ahmed and A. Hussein, "Behavior of Eccentrically Loaded RC Columns Strengthened with FRP," *World academy of Science Engineering and Technology*, vol. 68, pp. 2177–2186, 2012.

[7] H. S. Ahmed, A. Allawi, and R. Hindi, "Experimental Investigation of Composite Circular Encased GFRP I-Section Concrete Columns under Different Load Conditions," *Engineering, Technology & Applied Science Research*, vol. 14, no. 5, pp. 17286–17293, Oct. 2024, https://doi.org/10.48084/etasr.8521.

[8] M. Abdulkhaliq and A. H. Al-Ahmed, "Behavior of GFRP Reinforced-Concrete Bubbled One-Way Slabs by Encased Composite Steel I-Sections," *Engineering, Technology & Applied Science Research*, vol. 14, no. 5, pp. 16701–16712, Oct. 2024, https://doi.org/10.48084/etasr.8123.

[9] M. G. Abduljawad and A. H. Albayati, "Effect of Adding Steel and Glass Fibers on the Mechanical Properties and the Thickness of Rigid Concrete Pavements," *Journal of Engineering*, vol. 31, no. 5, pp. 172–188, May 2025, https://doi.org/10.31026/j.eng.2025.05.10.

[10] H. A. Hussein and A. I. Said, "Experimental Investigation of GFRP-Reinforced Hollow Square Concrete Column," *Journal of Engineering*, vol. 30, no. 06, pp. 108–124, Jun. 2024, https://doi.org/10.31026/j.eng.2024.06.07.

[11] M. A. Golham and A. H. A. Al-Ahmed, "Strengthening of GFRP Reinforced Concrete Slabs with Openings," *Journal of Engineering*, vol. 30, no. 01, pp. 157–172, Jan. 2024, https://doi.org/10.31026/j.eng.2024.01.10.

[12] T. H. Ibrahim and A. A. Allawi, "The Response of Reinforced Concrete Composite Beams Reinforced with Pultruded GFRP to Repeated Loads," *Journal of Engineering*, vol. 29, no. 01, pp. 158–174, Jan. 2023, https://doi.org/10.31026/j.eng.2023.01.10.

[13] M. Tavakol and H. Haji Kazemi, "Comparative assessment of concrete columns reinforced with hybrid steel-GFRP, GFRP, and steel bars under cyclic lateral loading," *Structures*, vol. 71, Jan. 2025, Art. no. 108034, https://doi.org/10.1016/j.istruc.2024.108034.

[14] B. Sinani and M. Barfed, "Analysis of Rectangular Concrete Columns with Hybrid Frp-Steel Bars," *UBT International Conference*, Oct. 2019, https://doi.org/10.33107/ubt-ic.2019.188.

[15] H. Tobbi, A. S. Farghaly, and B. Benmokrane, "Concrete Columns Reinforced Longitudinally and Transversally with Glass Fiber-Reinforced Polymer Bars," *ACI Structural Journal*, vol. 109, no. 4, pp. 551–558, 2012, https://doi.org/10.14359/51683874.

[16] A. De Luca, F. Matta, and A. Nanni, "Behavior of Full-Scale GFRP Reinforced Concrete Columns under Pure Axial Load," *ACI Structural Journal*, vol. 107, no. 5, pp. 589–596, 2010.

[17] M. N. S. Hadi and J. Youssef, "Experimental Investigation of GFRP-Reinforced and GFRP-Encased Square Concrete Specimens under Axial and Eccentric Load, and Four-Point Bending Test," *Journal of Composites for Construction*, vol. 20, no. 5, Oct. 2016, Art. no. 04016020, https://doi.org/10.1061/(ASCE)CC.1943-5614.0000675.

[18] M. Z. Afifi, H. M. Mohamed, and B. Benmokrane, "Axial Capacity of Circular Concrete Columns Reinforced with GFRP Bars and Spirals," *Journal of Composites for Construction*, vol. 18, no. 1, Feb. 2014, Art. no. 04013017, https://doi.org/10.1061/(ASCE)CC.1943-5614.0000438.

[19] H. El Chabib, M. Nehdi, and M.-H. El Naggar, "Behavior of SCC confined in short GFRP tubes," *Cement and Concrete Composites*, vol. 27, no. 1, pp. 55–64, Jan. 2005, https://doi.org/10.1016/j.cemconcomp.2004.02.045.

[20] F. Micelli and A. Nanni, "Durability of FRP rods for concrete structures," *Construction and Building Materials*, vol. 18, no. 7, pp. 491–503, Sep. 2004, https://doi.org/10.1016/j.conbuildmat.2004.04.012.

[21] Y. Zhan, G. Wu, and L.S. Yang, "Experimental Investigation of the Behavior of a Lattice Steel Column Repaired with Pultruded GFRP Profiles," *Journal of Performance of Constructed Facilities*, vol. 29, no. 4, Aug. 2015, Art. no. 04014094, https://doi.org/10.1061/(ASCE)CF.1943-5509.0000600.

[22] C. Campian, Z. Nagy, and M. Pop, "Behavior of Fully Encased Steel-concrete Composite Columns Subjected to Monotonic and Cyclic Loading," *Procedia Engineering*, vol. 117, pp. 439–451, Jan. 2015, https://doi.org/10.1016/j.proeng.2015.08.193.

[23] A. K. P. K. Pandey, M. Dada, M. L. Patton, and D. Adak, "A comparative review on the structural behaviour of GFRP rebars with conventional steel rebars in reinforced concrete columns," *Innovative Infrastructure Solutions*, vol. 9, no. 10, Sep. 2024, Art. no. 373, https://doi.org/10.1007/s41062-024-01686-0.

[24] M. G. Elshamandy, A. S. Farghaly, and B. Benmokrane, "Experimental Behavior of Glass Fiber-Reinforced Polymer-Reinforced Concrete Columns under Lateral Cyclic Load," *ACI Structural Journal*, vol. 115, no. 2, pp. 337–349, Mar. 2018, https://doi.org/10.14359/51700985.

[25] *ASTM A370-17 Standard Test Methods and Definitions for Mechanical Testing of Steel Products*. USA: ASTM International, 2017.